PERGAMON

Journal of Geodynamics 32 (2001) 205–229

JOURNAL OF
GEODYNAMICS

www.elsevier.nl/locate/jgeodyn

The astronomical connection of terrestrial evolution: crustal effects of post-3.8 Ga mega-impact clusters and evidence for major 3.2±0.1 Ga bombardment of the Earth–Moon system

Andrew Y. Glikson

Research School of Earth Science, Institute of Advanced Study, Australian National University, Canberra, ACT 0200, Australia

Received 1 March 2000; received in revised form 5 June 2000; accepted 26 April 2001

Abstract

It is accepted that during the Late Heavy Bombardment (LHB—4.2–3.8 Ga) in the Solar system, as preserved on the Moon, the terrestrial upper mantle-crust system was dominated by interactions between internal mantle processes and extraterrestrial impacts, and that following this period, the impact flux decreased by two orders of magnitude, from 4–9×10^{-13} km^{-2} $year^{-1}$ to 3.8–6.3×10^{-15} km^{-2} $year^{-1}$ (for asteroids $Dc>=18$ km), a rate consistent with a cratering rate of 5.9±3.5×10^{-15} km^{-2} $year^{-1}$ estimated for near-Earth asteroids (NEA) and comets. Geology being a geocentric science, the assumption is generally made that from about 3.8 Ga the impact factor can be neglected in the context of models of crustal evolution, including the emergence of early continental nuclei and plate tectonics. This paradigm is questioned in this paper. From the observed minimum number of 6 continental impact structures with $Dc>=100$ km [Vredefort (300 km); Sudbury (250 km); Chicxulub (170 km); Woodleigh (120 km); Manicouagan (100 km); Popigai (100 km)], assuming an Earth surface occupied by time-integrated $>=80\%$ ocean crust since 3.8 Ga, the lower limit of post-LHB impacts is deduced at $>=30$ craters with $Dc>=100$ km and $>=10$ craters with $Dc>=250$ km. From the lunar crater counts and the present-day asteroid flux the impact incidence was likely to have been higher by an order of magnitude, with a possible decline in the impact frequency of the largest bodies $Dp>=20$ km. Evidence for maria-scale impact basins in the Archaean emerges from 3.24 Ga-old impact vapor condensation-fallout layers in the Barberton greenstone belt, Transvaal, pointing to multiple oceanic impact basin of $Dc>=400$ km. This impact cluster falls within error from the c. 3.18 Ga impact peak documented by lunar spherules—suggesting a mid-Archaean impact cataclysm in the Earth–Moon system. Models of crustal evolution need to account for the inevitable magmatic and tectonic consequences of these events, particularly on impacted geothermally active oceanic

E-mail address: andrew.glikson@anu.edu.au

0264-3707/01/$ - see front matter
PII: S0264-3707(01)00029-1

crust and lithosphere. A combination of the internal heat engine and the impact factors is capable of accounting for the early sialic nuclei, for the spatial and temporal localization of major faulting and rifting events, and for ensuing plate tectonic patterns.

1. Post-LHB impact rates and extraterrestrial bombardment episodes

Current models of crustal tectonic and magmatic evolution neglect the consequences of impact by very large asteroids and comets in the inner solar system in the wake of the Late Heavy Bombardment, assuming that the decline from a flux of $4–9\times10^{-13}$ km^{-2} year^{-1} (for craters $Dc>=18$ km) to a flux of $3.8–6.3\times10^{-15}$ km^{-2}·year^{-1} (for craters $Dc>=20$ km) (Grieve and Dence, 1979; Baldwin, 1985; Ryder, 1990) renders the mega-impact factor of little relevance. Post-LHB impact rates estimated from lunar and terrestrial crater counts are of the same order of magnitude as the cratering rate of $5.9\pm3.5\times10^{-15}$·km-2 year^{-1} (for craters $Dc>=20$ km) estimated from astronomical observations of near-Earth asteroids (NEA) and comets (Shoemaker and Shoemaker, 1996). Combining these rates with crater size vs cumulative size frequency relationships approximating $N\infty Dc^{-1.8}$ to $N\infty Dc^{-2.0}$ (Dc = crater diameter; N = cumulative number of craters with diameters larger than Dc), implies the formation of more than 53 craters of $Dc>=300$ km, and more than 19 craters of $Dc>=500$ km since ~3.8 Ga nearly two orders of magnitude higher than the preserved record (Table 1; Figs. 1, 2, 3).

According to W. Bottke (personal communication, 1999) the size distribution relationship $N\infty D^{-1.8}$, is probably only valid for craters <100 km. NEAs in the range of $Dp=0.1–5.0$ km correspond better to the relation $N\infty Dp^{-2.0}$, consistent with young cratered surfaces on the terrestrial planets. For 43 NEAs with $Dp>12$ km an observed relation $N\infty Dp^{-2.73}$, suggests a decline in the number of the largest impactors relative to smaller bodies, with implications for craters of $Dc>=100$ km. The frequency of the largest asteroids, such as Eros (long axis $Dp=27$ km), Swift Tuttle ($Dp=24$ km) and Ganymede ($Dp=39$ km) is uncertain, but a preliminary estimate suggests about or over 12 impacts by bodies of this scale since the LHB. The role of cometary impacts is not included in this estimate.

Comparing the above estimates with the preserved terrestrial cratering record documented to date, the minimum extraterrestrial impact incidence for craters $Dc>=100$ km is defined by the 6 observed impact structures of $Dc>=100$ km [Vredefort (300 km); Sudbury (250 km); Chicxulub (170 km); Woodleigh (120 km); Manicouagan (100 km); Popigai (100 km)], which struck continental crust. Assuming an Earth surface occupied by >80% time-integrated oceanic crust in post-LHB times, a minimum number of 30 craters with $Dc>100$ km and 10 craters $Dc>=250$ km is deduced (Table 1). Several suggested impact structures remain unconfirmed, for example large circular structures in Fennoscandia (Nunjes—$Dc\sim400$ km; Uppland—$Dc\sim300$ km; Marras—$Dc\sim250$ km) (Pesonen, 1996), and several Australian structures of possible impact origin (Gorter, 1998).

The impact incidence requires re-examination of the terrestrial crustal record in view of the regional to global magmatic, seismic and tectonic consequences predicted by Green (1972, 1981), Grieve (1980), Roddy et al. (1987) and others. Attempts at examining the possibility that major magmatic-tectonic Precambrian episodes may represent the effects of mega-impact clusters (Glikson, 1993, 1996, 1999) are complicated by possible sampling bias. However, from available

Table 1
Post-LHB terrestrial impact rates[a] and estimated minimum numbers of craters on several scales

Estimated cratering rate = $R \times 10^{-15}$ km^{-2} year^{-1} craters with $Dc >= 20$ km	Estimated number of craters of size $>= Dc$ (in km) during 3.8 Ga to the present				
_	$Dc >= 20$	$Dc >= 100$	$Dc >= 300$	$Dc >= 500$	$Dc >= 1000$
$R = 4.3 \pm 0.4$ (Ref. 1)	8300	390	45	17	4
$R = 3.8 \pm 1.9$ (Ref. 2)	7350	320	36	14	3
$R = 6.3 \pm 3.2$ (Ref. 3)	12 200	560	74	24	6
$R = 5.6 \pm 2.8$ (Ref. 4)	10 840	470	56	20	5
$R = 5.9 \pm 3.5$ (Ref. 5)	11 450	520	60	22	6
$R = 5.5 \pm 2.7$ (Ref. 6)	10 630	460	54	19	5
R_m (mean) = 5.23	10 130	450	53	19	5
A	2026	90	11	4	1
B	8104	363	42	15	4
C	39	6	2 with $Dc >= 250$	N.A.	N.A.
D		30	10	N.A.	N.A.
E	0.38	1.3	3.8	N.A.	N.A.
F	1.9	6.6	18	N.A.	N.A.

a Based on literature estimates for craters with $Dc >= 20$ km, and on projected crater numbers for craters with $Dc >= 100$ km, $Dc >= 300$ km, $Dc >= 500$ km, and $Dc >= 1000$ km, projected from crater size vs. cumulative crater size plots with $N \infty Dc^{-1.8}$. Numbers of craters are rounded. The number of craters with $D >= 250$ km assumes Morokweng to be a ca. 340 km-diameter crater (Corner et al., 1997) and Sudbury as a 200–250 km-diameter crater (Deutsch, 1998). Ref. 1. Terrestrial cratering rate equivalent to the lunar cratering rate ~3.2 Ga; asteroid impact velocities assumed (Shoemaker and Shoemaker, 1996). Ref. 2. Proterozoic impact rate estimated from Australian impact structures (Shoemaker and Shoemaker, 1996). Ref. 3. Phanerozoic impact rates estimated by extrapolation from impact structures $Dc >= 10$ km in central United States (Shoemaker and Shoemaker, 1996). Ref. 4. Cratering rate since 120 Ma (Grieve and Shoemaker, 1994). Ref. 5. Present cratering rate estimated from astronomical surveys (Shoemaker and Shoemaker, 1996). Ref. 6. Terrestrial cratering rate for craters of $Dc >= 20$ km (Grieve and Pesonen, 1996). A. Predicted number of continental craters. B. Predicted number of oceanic craters. C. Number of observed continental craters. D = Absolute minimum number of craters deduced for the entire Earth as based on C. E. Percent observed to predicted craters for entire Earth surface. F. Percent observed to predicted craters for a time-integrated continental crust area.

data major greenstone/granite-forming periods occur about ~3.47, ~3.24, ~3.0 and ~2.7 Ga, an episodicity not yet explained by purely endogenic models. In the present paper, this line of investigation is pursued further with respect to the origin of Archaean sialic nuclei and the spatial-temporal distribution of plate tectonic patterns.

2. Implications of the lunar impact evidence

The so-called Late Heavy Bombardment (LHB), broadly defined at 4.2–3.8 Ga, may represent the tail-end of planetary accretion or, alternatively, a temporally distinct bombardment episode 3.95–3.80 Ga (Ryder, 1990, 1991). Some of the largest lunar maria basins contain low-Titanium basalts which likely represent impact-triggered volcanic activity (Ryder, 1997), including Mare

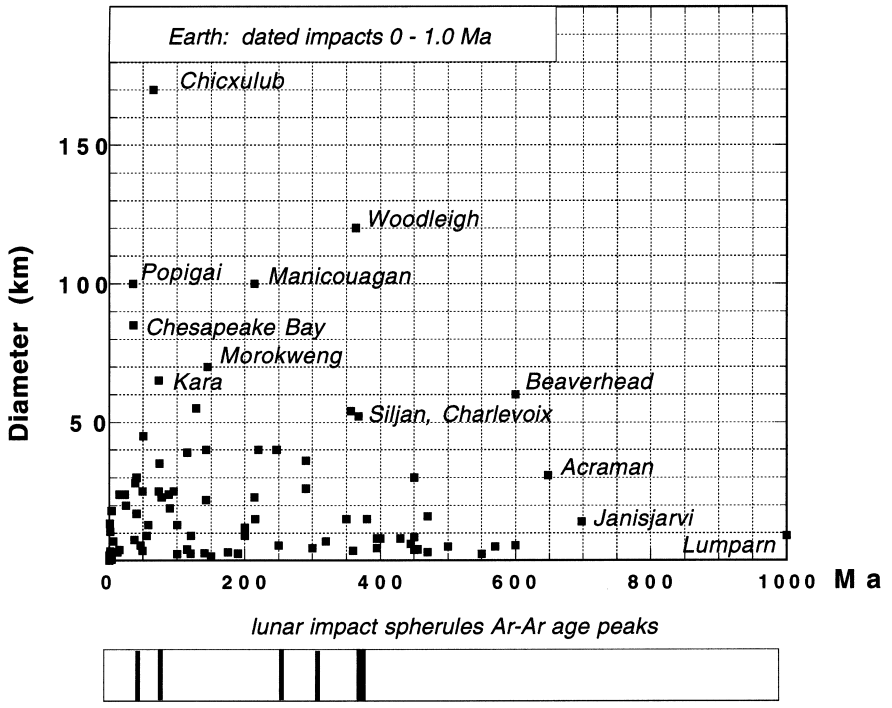

Fig. 1. Plots of extraterrestrial impact structures isotopically dated in the range of up to 1.0 Ga (based on Grieve, 1997, Geological Survey of Canada database). Plotted also are some of the main Ar–Ar isotopic lunar impact event peaks based on Culler et al. (2000).

Imbrium (3.86±0.02 Ga) and associated 3.85±0.03 Ga-old K, REE, and P-rich-basalts (KREEP) (BVTP, 1981). Similar relationships between impact and volcanic activity may pertain in Oceanus Procellarum (3.29–3.08 Ga basalts) and in Hadley Apennines (3.37–3.21 Ga basalts) (BVTP, 1981). The likelihood of impact-volcanic relationships on the Moon gains support from the recent laser 40Ar/39Ar analyses of lunar impact spherules from sample 11199 (Apollo 14, Fra Mauro Formation) (Muller, 1993; Culler et al., 2000). Impact events tentatively indicated by the lunar spherule data include 3.87, 3.83, 3.66, 3.53, 3.47 Ga peaks. A significant age spike is indicated at 3.18 Ga, i.e. near the boundary between the Late Imbrian lunar era (3.9–3.2 Ga) and the post-mare Eratosthenian lunar era (3.2–1.2 Ga) (Fig. 2), as defined by the cratering record (Wilhelms, 1987) (Fig. 3). Some 34 lunar impact spherules yield a mean age of 3188±198 Ma with a median age at 3181 Ma, whereas 7 spherule ages with error <100 m.y. yield a mean age of 3178±80 Ma and a median at 3186 Ma (Fig. 1)—discussed further in this paper in connection with the 3.24–3.227 Ga impact cluster indicated by impact condensate spherule units in the Barberton Mountain Land, Transvaal.

Tentative correlations between the lunar spherule data and terrestrial events include the following (Figs. 1 and 2): (1) The sharp 3.53 and 3.47 Ga maxima closely correlate with peak magmatic activity associated with the formation of Archaean greenstone–granitoid systems in the Pilbara (Western Australia), Kaapvaal (Transvaal), Zimbabwe and India. (2) The 1.8 Ga "high" (including relatively precise spherule ages of 1813±36.3) occurs within error from the 1.85 Ga age

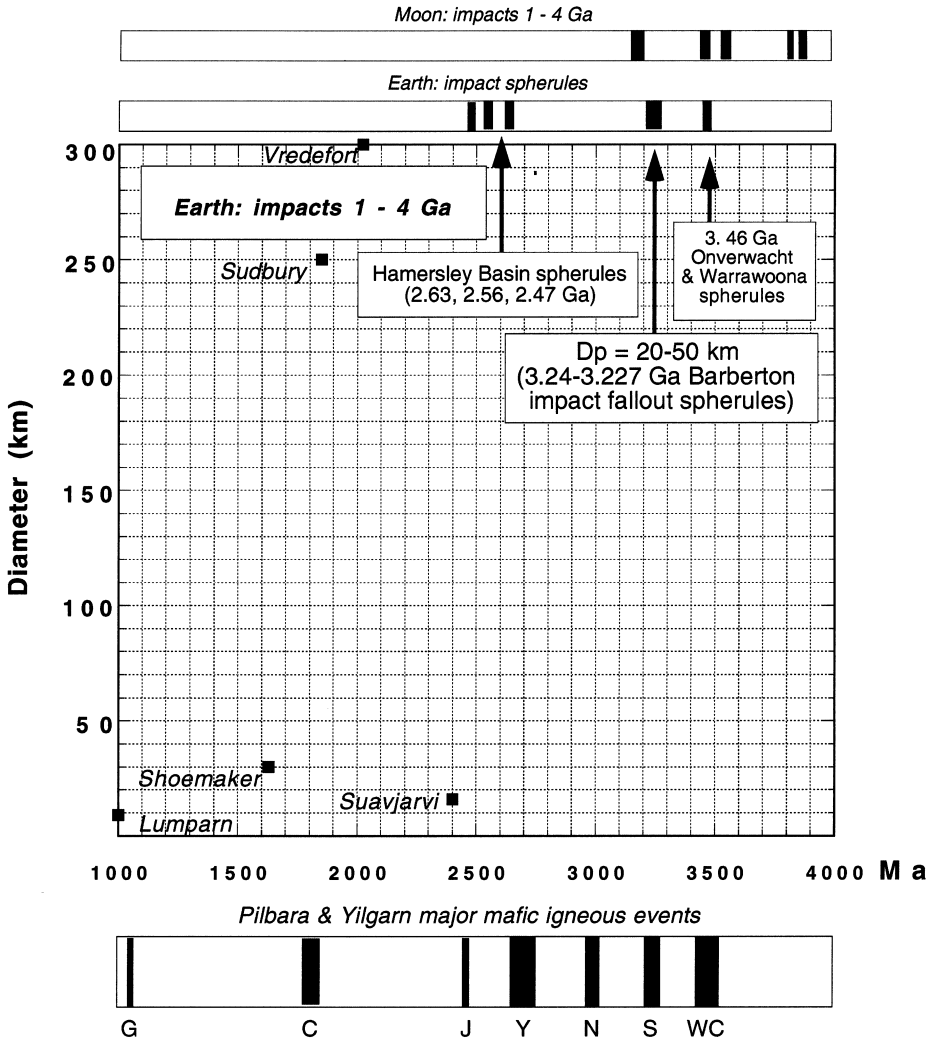

Fig. 2. Plots of extraterrestrial impact structures isotopically dated in the range of 1.0–4.0 Ga (based on Grieve, 1997, Geological Survey of Canada database). Plotted also are (1) ages of terrestrial impact spherules (after Simonson and Hassler, 1997 and Byerly and Lowe, 1994); (2) some of the main Ar–Ar isotopic lunar impact event peaks based on Culler et al. (2000); (3) major mafic-ultramafic igneous events in the Pilbara, Yilgarn and Musgrave blocks, Western Australia. WC—Warrawoona and Cooterunah Groups, Pilbara (3.42–3.51 Ga); S—Strelley Group, Pilbara (3.24 Ga); N—Negri Volcanics, Pilbara (2.99–2.95 Ga); Y—Yilgarn greenstones (2.72–2.67 Ga); J—Jimberlana dyke suite, Yilgarn (2.45–2.42 Ga); C—mafic volcanics of the Capricorn/Gascoyne belt ($\sim$1.8 Ga) straddling the Pilbara and Yilgarn cratons; G—Giles mafic-ultramafic intrusive complex, Musgrave Block (1.08 Ga).

of the >250 km-diameter Sudbury impact structure, Ontario (Grieve, 1997). (3) Two of the shallower age "rises" overlap the age of impact spherules in the Hamersley Basin, Western Australia, including a 2.56 Ga spherule marker in the Wittenoom Formation (carbonates) (Plate A2) and a 2.47 Ga spherule unit in the Dale Gorge member (banded ironstones) (Simonson, 1992; Simonson and Hassler, 1997). (4) The 1.08 Ga peak parallels the emplacement of the large layered

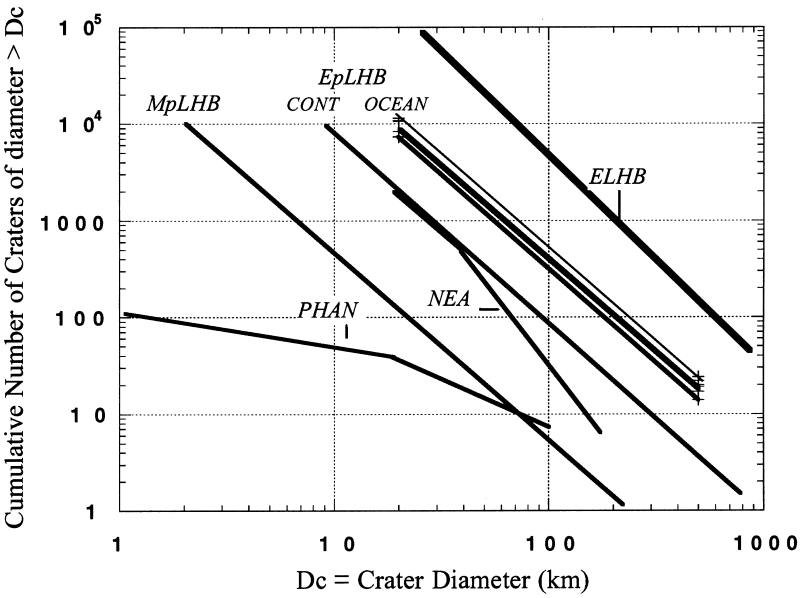

Fig. 3. Crater size vs. cumulative frequency plots for post-LHB times in Earth–Moon system. MpLHB—post-lunar maria craters and post-Martian plains craters (after Barlow, 1990). NEA—crater distribution extrpolated from observed Near-Earth Asteroids ($Dc = 20$ Dp). PHAN—Phanerozoic impact rates after Grieve and Dence (1979), showing loss of smaller craters. EpLHB—average Earth cratering rate based on Table 1 and extrapolated to entire Earth surface on basis of number of $\geqslant 20$ km-diameter craters and cumulative crater vs size-frequency relationships parallel to those of MpLHB; CONT—mean cratering rate on time-integrated continental crust ($\sim 20\%$ of Earth's surface). OCEAN—mean cratering rate on time-integrated ocean crust ($\sim 80\%$ of Earth's surface). E-LHB—Late heavy bombardment of Earth, extrapolated from lunar data of Barlow (1990).

mafic-ultramafic Giles Complex, central Australia (Glikson et al., 1995). Notable in their absence are spherule age peaks corresponding to the 2023 Ma 300 km-diameter Vredefort impact structure. The huge c.2.7 Ga terrestrial greenstone-granitoid events (Glikson, 1996, 1999) are not mirrored by any corresponding spherule ages although the maximum age of the Jeerinah spherule unit (2.63–2.68 Ga, Simonson and Hassler, 1997) occurs near these events.

Nine lunar spherules were dated with errors of less than 20 m.y., allowing comparisons with terrestrial isotopic ages of similar precision. These include (1) 3872.1 ± 11.2 and 3807.4 ± 14.5 Ma ages corresponding to the Late Heavy Bombardment; (2) 3542 ± 11.4 and 3475.8 ± 15 Ma ages correlated with major Archaean greenstone forming events in the Pilbara and Transvaal; and 3186.2 ± 12.1, 352.6 ± 6.6 , 304.6 ± 17, 51.4 ± 4.0 Ma.

The lunar spherule age data reflect the late Devonian impact cluster (Woodleigh, Western Australia (Mory et al., 2000), $D = 120$ km, 364 ± 8 Ma (T. Uyssal, personal communication, 2000) Charlevoix, Quebec, 367 ± 15, $D = 54$ km; Siljan, Sweden, 368 ± 11 Ma, $D = 52$ km; Alamo breccia, western Nevada, of Frasnian-Fammenian age, including impact spherules, shocked quartz and Ir anomalies; Ternovka, Ukraine, 350 Ma, $D = 15$ km; Kaluga, Russia, 380 ± 10, $D = 15$ km; Ilynets, Ukraine, 395 ± 5 Ma, $D = 4.5$ km; Elbow, Saskatchewan, 395 ± 25 Ma, $D = 8$ km) and contemporaneous Frasnian-Famennian and end-Devonian extinctions of a range of rugose coral reefs, trilobites, ammonoids, brachiopods and chonodont species. The late Devonian events may be paralleled by a precise lunar spherule age of 352.6 ± 6.6 Ma age and a cumulative "high" of 11

spherule ages with errors >100 m.y. (Fig. 1). Other correlations are indicated by lunar spherule ages of 303 Ma (Carboniferous–Permian boundary), 251 Ma (Permian–Triassic boundary), 103 Ma, 64–71 Ma (Cretaceous–Tertiary boundary), 52 and 38–32 Ma (late Eocene impacts and extinction).

3. Origin of Archaean sialic nuclei

The history of Precambrian crustal research is replete with examples of prevailing dogmas questioned by few dissenting voices. Until the late-seventies it was widely assumed an early Archaean granitic continental crust universally underlies the supracrustal greenstone sequences, as indicated by the literature on the North Atlantic shield (Sutton, 1971; Bridgwater and Collerson, 1976), in Canada (Donaldson and Jackson, 1965; Ayres, 1974; Henderson, 1975; Baragar and McGlynn, 1976), South Africa (Hunter, 1970, 1974), Western Australia (Binns et al., 1976; Gee, 1976; Archibald and Bettenay, 1977; Hickman, 1981) and South India (Ramakrishnan et al., 1976; Chadwick et al., 1978). From the late sixties an increasing number of papers appeared supporting analogies between greenstone sequences and modern arc-trench or back-arc domains, a class of models supported by (1) geochemical and isotopic parameters (Folinsbee et al., 1968; Baragar and Goodwin, 1969; Glikson, 1970, 1971; Arth and Hanson, 1975), and (2) the common occurrence of mafic and ultramafic enclaves within granitic batholiths and early gneiss terrains (Engel, 1966; Glikson, 1970, 1971, 1984; Anhaeusser, 1973; Naqvi, 1976) However, the detection of early Sm-Nd signatures in Archaean mafic and ultlramafic rocks in the Pilbara Craton (Gruau et al., 1987), and of high initial U/Pb ratios and zircon xenocrysts in Yilgarn Kalgoorlie-Norseman greenstones (Oversby, 1975; Compston et al., 1986), pointed to existence of pre-greenstones sialic materials, although not necessarily to continuously underlying continental crust.

Since the seventies the literature on the Archaean became dominated by plate tectonic-centred or modified plate tectonic models (Tarney et al., 1976; Windley, 1977; Kroner, 1981; Card, 1990; Krapez, 1993; Myers, 1995; de Wit, 1982, 1998), a trend continuing at present. Few non-unformitarian views point out fundamental distinctions between Archaean greenstone-granite terrains and modern arc-trench domains [Glikson, 1980; 1993, 1996, 1999; Hamilton, 1998, Drury, 1999 (pp. 122–125), and the present paper].

The proliferation of models on the origin of early continental nuclei, increasing instead of decreasing despite the rapidly growing database, reflects a methodological impasse in Archaean research. An understanding of Archaean geotectonic patterns is complicated by the imbalance between temporal and spatial controls, namely the large body of accurate isotopic age data is contrasted with the near-absence of palaeomagnetic controls. However, two principal sets of observations in Archaean terrains are difficult to reconcile with a Mesozoic–Cainozoic-type plate tectonic model: (1) development of multi-cyclic volcanic-sedimentary greenstone belt depositories over periods up to $\sim 300 \times 10^6$ years-long, contrasted with arc-trench histories which are shorter by about an order of magnitude, and (2) the episodic intermittent nature of magmatic-tectonic events. Neither feature is consistent with the shorter life span of circum Pacific-type marginal basins, or continuous build up of accretionary wedge assemblages. Where such fundamental dilemmas arise, the basic assumptions inherent in the uniformitarian models require reassessment.

4. Problems with Archaean plate tectonic models

The contrast between Archaean plate tectonic-type models and the fundamental differences between greenstone-granite terrains and Cainozoic–Mesozoic arc-trench domains (Hamilton, 1998) underpins the impasse reached in the understanding of the early Earth. The current consensus is expressed by de Wit (1998): "The verdict is that there is a robust consensus on the validity of using plate tectonic boundary processes to decipher the late Archaean rock record; and it also confirms that such processes dominated the early Archaean". This school of thought stems to a large extent from geochemical and isotopic evidence for operation of two-stage mantle melting-type processes in the Archaean, including the dominance of the tonalite-trondhjemite-granodiorite (TTG) plutonic assemblage (Glikson and Sheraton, 1972; Jahn et al., 1980), interpreted by many workers in terms of crustal recycling triggered by the basalt-eclogite transformation (Arth and Hanson, 1975; Glikson and Lambert, 1976). Implicit in these models is the assumption that similar petrological melting/differentiation processes necessarily require similar geotectonic settings. The advocacy of plate tectonic models was developed in the context of local overthrust tectonics, for example in anticlinal hinges in the Barberton greenstone belt, Eastern Transvaal, where relic Archaean oceanic crust was thought to exist (Engel, 1966; Glikson, 1971, 1972; de Wit, 1982; de Wit et al., 1987). More recently, the general agreement, with some exceptions, between U–Pb zircon ages of felsic volcanic units in the Onverwacht Group and stratigraphic sequences (Kamo and Davis, 1994; Byerly et al., 1995; Kroner et al., 1996) has vindicated some of the principal elements of the stratigraphy of the Barberton greenstone belt as originally mapped by C.R. Anhaeusser, M.J. Viljoen and R.P. Viljoen in the sixties and the seventies (Viljoen and Viljoen, 1971; Anhaeusser, 1973).

A plate tectonic origin of Archaean greenstone-granite systems has been supported by many workers in view of a perceived lateral age zonation in Archaean cratons, suggestive of circum-Pacific type accretion. For example, general eastward younging in the Yilgarn Craton (Myers, 1995), westward younging in the Pilbara craton (Barley, 1993), and southward younging in the Superior Craton (Card, 1990) have been suggested. However, such trends are complicated by (1) isotopic signatures of older crust within younger zones, for example in the western Pilbara (Sun and Hickman, 1998) and the Superior Province (R. Loucks, personal communication, 1999), and (2) superposition of younger events on older crust, for example of ~2.7 Ga events on older terrains in the northern Superior Province (Card, 1990) and in the Western Yilgarn (Myers, 1995). The following evidence is difficult to reconcile with interpretations of greenstone belts in terms of accretionary wedge models:

1. Archaean supracrustal depositories in the Pilbara and Barberton greenstone belts consist of multiple superposed generations of volcanic-sedimentary assemblages, separated from one another by unconformities and paraconformities, and spanning combined periods of several 10^8 years. In the eastern Pilbara Craton these include the Cooterunah Group (~3.51 Ga), Warrawoona Group (3.48–3.42 Ga), Sulphur Springs Group (~3.24 Ga), and Whim Creek Group (~3.0 Ga). Major felsic plutonic magmatic events broadly overlap these intervals, including several granitoid components of pre-3.5 Ga age, ~3.47–3.42, ~3.3, ~3.24 and ~3.0 Ga. In the Barberton greenstone belt the Onverwacht Group contains vertically superposed mafic-ultramafic and felsic volcanic units formed intermittently between 3.55–3.3

Ga and overlain by clastic sediments and felsic volcanics of the Fig Tree and Moodies Groups (Kamo and Davies, 1994; Byerly et al., 1995) (Plate 5).

2. The episodic nature of Archaean magmatism is difficult to reconcile with either ongoing or short-term intermittent plate tectonic processes. As some of these episodes are correlated between several Archaean cratons, they may hint at global thermal pulsations whose origin remains unknown and subject of models such as plume tectonics (Campbell and Griffiths, 1992) or 'plume impact' (Courtillot et al., 1999).
3. Assumptions of seamless to intermittent Archaean crustal accretion/subduction processes, analogous to Mesozoic-Phanerozoic plate tectonic patterns, are faced with a crustal volume problem. For example, in a modern-type geotectonic framework with an oceanic ridge system of ~20 000 km total length, oceanic and continental crustal thicknesses, and mid-ocean accretion rate of 3.2 km^2 $year^{-1}$, crustal accretion by two-stage mantle melting processes post-LHB would result in formation of continental crust over the entire Earth surface (Glikson, 1983). The enigma is exacerbated by predicted higher rates of crustal accretion expected in the Archaean due to higher heat flow (Lambert, 1975). Green (1981) suggested the basalt-eclogite transformation, and thus two-stage melting processes, were arrested by the higher Archaean geotherms. Likewise, subduction and assimilation of sial, which could account for the volume problem, are unlikely due to (1) buoyancy of sial under high heat flow conditions, and (2) geochemical and isotopic parameters indicative of temporally repeated melt extraction from pristine mantle (McCulloch and Bennett, 1994).

The theoretical questions which confront Archaean plate tectonic models are corroborated by field evidence. Based on a life-long experience in the study of Phanerozoic circum-Pacific arc-trench and accretionary wedge terranes, Hamilton (1998) offers perspectives which eluded advocates of Archaean plate tectonic models, observing: "The granite and greenstone terrains that typify Archaean cratons represent a distinct type of magmatic and tectonic development within the span of 3.6–2.6 Ga. They have no modern analogues, and they were not product of plate tectonics." (p. 144), and "Granite and greenstone terrains typify Archaean upper crust and have no post-Archaean structural and magmatic analogues." (p.145). At least in the Archaean terrains with which I am acquainted I have not seen imbricately thrusted melange-ophiolite assemblages typical of accretionary wedges.

The question is complicated by occurrences of post-Archaean greenstone-like belts, for example ~2.1 Ga Birimian belts, ~1.8 Ga Snow Lake and Flin-Flon belt, the Sierra Nevada batholiths with their supracrustal enclaves (Hietanen, 1975), and the Roche Verde assemblage in Chile (Tarney et al., 1976). In assessing similarities and differences between these supracrustal belts and Archaean greenstone belts, it must be borne in mind that the latter are far from uniform and do not conform to any single class. For example, there is little in common between the komatiite-rich Barberton greenstones (Viljoen and Viljoen, 1971; Anhaeusser, 1973) and late Archaean intra-sialic supracrustals of the Slave Province, Northwestern Territories (Padgham, 1992).

Within multi-stage Archaean greenstone belts, younger supracrustal cycles may locally overlap older cratonic blocks. On the other hand, some the older greenstone sequences (e.g. Warrawoona Group, Onverwacht Group, Sebakwian Group) may represent slices of inter-sialic simatic crust. If so, the Archaean sima is distinguished from modern oceanic crust by the abundance of high-Mg to peridotitic komatiite, felsic volcanic intercalations, chert and banded ironstones. These

assemblages need not necessarily have formed along spreading ocean ridges. Nor do xenocrystic zircons in the early greenstone units (Compston et al., 1986) necessarily indicate a contiguous sub-greenstone continental-scale sialic crust, but may represent isolated granitic blocks, and/or derivation of the xenocrysts from sediments shed from older neighbouring cratonic blocks. Examples of the latter may be the ~3.65 Ga Swaziland gneisses (Kaapvaal Craton) and de Gray gneisses (Pilbara Craton) of similar ages (I.R. Williams, personal communication, 1999) which fringe, but may not necessarily underlie, neighboring greenstone belts. Archaean geotectonic frameworks may have consisted of numerous sialic blocks, or early nuclei, interspersed with rifted simatic troughs, a pattern whose confirmation requires the extension of palaeomagnetic methods further back in time.

The problems encountered with Archaean plate tectonic models hint at the potential importance of hitherto unaccounted-for factors, including the effects of asteroid and comet mega-impacts. Since 1986, evidence has been accumulating for the occurrence of spherulitic vapour condensate (microkrystite) fallout deposits within 3.24 Ga sediments of the Barberton greenstone belt, eastern Transvaal (Lowe and Byerly, 1986) (Plates 1–5). As this is the first established example of a major Archaean impact cluster, the evidence is discussed in further detail below.

5. Evidence of Archaean mega-impact clusters and terrestrial mare

Four spherule units have been identified in the Barberton greenstone belt (Lowe and Byerly, 1986; Lowe et al., 1989; Kyte et al., 1992; Byerly and Lowe, 1994; Byerly et al., 1995): S1—3474–3445 Ma ; S2—3243±4 Ma; S3, S4—3243–3227±4 Ma. Study of units S3 and S4 indicates (1) marked PGE anomalies with partly to largely modified chondritic patterns; (2) relic iridium nanonuggets located within sulfides; (3) Nickel-rich (<23% NiO) octahedral and quench-skeletal chromites (Plate 4) with extremely high levels of siderophile and chalcophile elements (Ni, Co, V, Zn)—a composition unique to spinels observed in impact vapour-condensate spherules contained

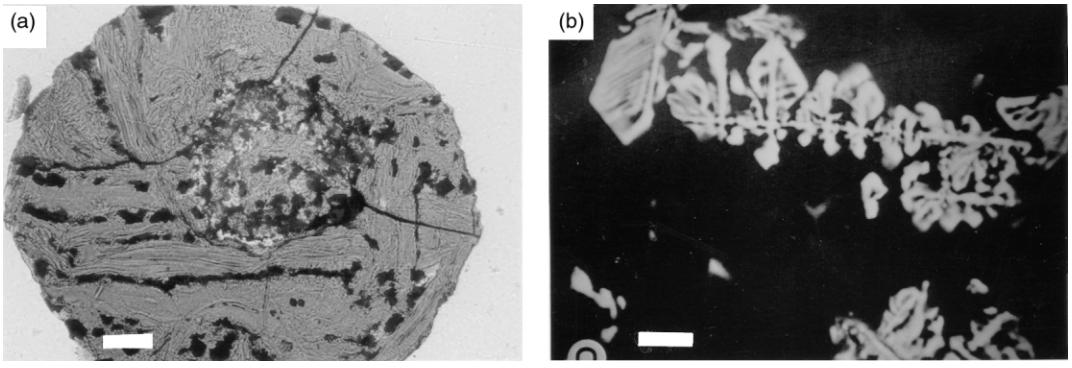

Plate 1. (a) An impact condensate fallout spherule replaced by chlorite sheafs and containing opaque Ni-rich chromites. Eocene-Oligocene spherulitic unit in carbonates at Massiniano, near Ancona, east Apennines. Scale bar—0.1 mm; (b) skeletal Ni-rich chromite from the above spherule, representing quench crystallisation within the original liquid droplet. Cross-nicols. Scale bar—0.001 mm. Courtesy of Alessandro Montanari.

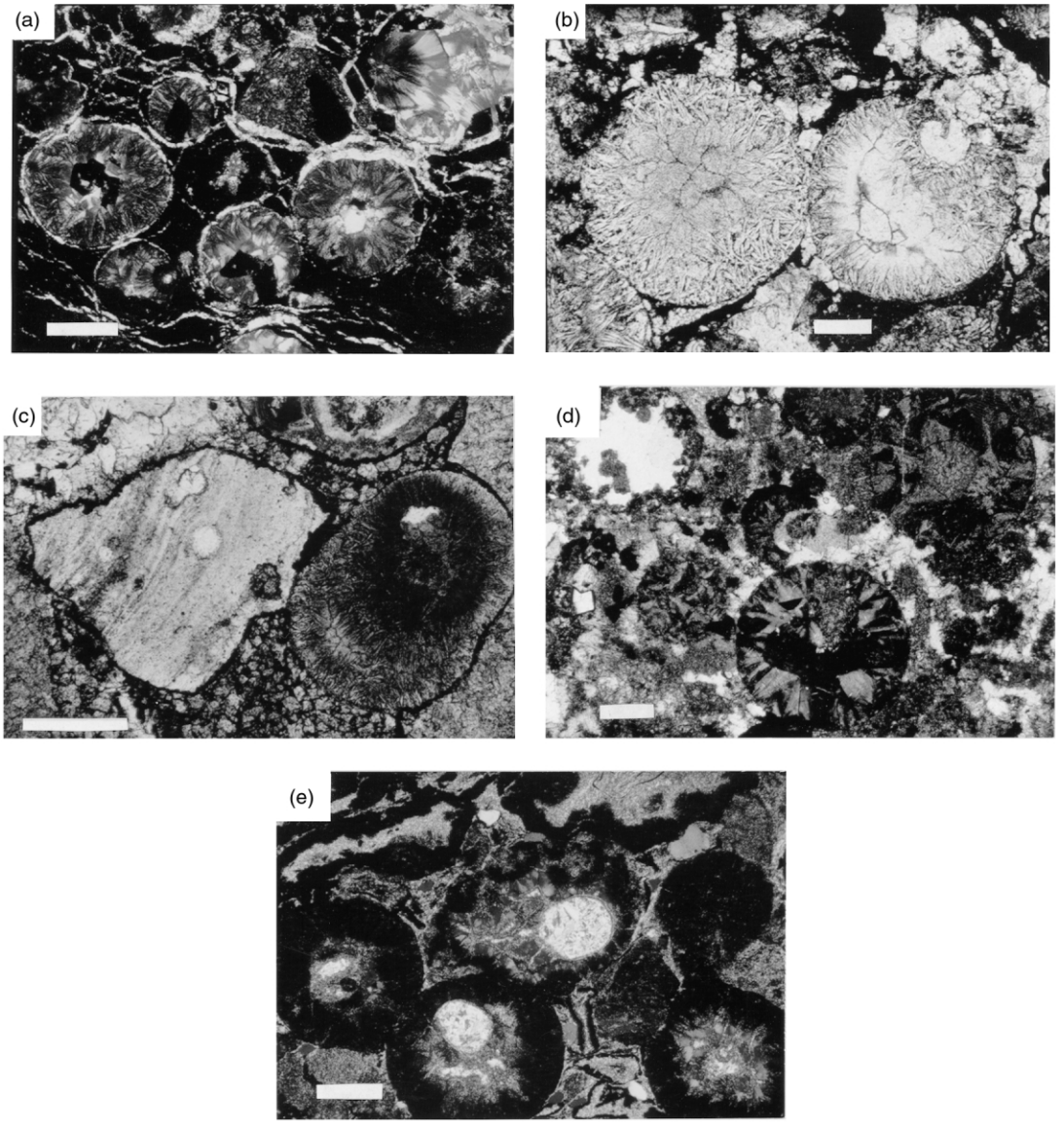

Plate 2. Impact condensate fallout spherules in the c. 2.56 Ga Wittenoom Formation and Carawine Dolomite, Hamersley Basin, Western Australia, and the Monteville Formation, Western Transvaal. (a) Spherulitic condensates from the Spherule Marker Bed, Bee Gorge Member, Wittenoom Formation, showing inward radiating fans of K-feldspar, with coarse carbonate crystals at spherule centres, set in clouded carbonate micrite. Cross-nicols. Scale bar—0.25 mm. (b) Plane polarised microphotograph of spherules as in A. Note the inward-radiating K-feldspar needles, mimicking quench crystallisation textures but which more likely represent devitrification features. (c) Twin spherule and flow-textured K-feldspar fragment from dolomite breccia (dolomixtite) of the Carawine Dolomite. Plane polarised light. Scale bar—0.5 mm. (d) Spherules with inward radiating chlorite, carbonate and quartz, Monteville Formation. Plane polarised light. Scale bar 0.5 mm. (e) Spherules with offset central bubbles filled with carbonate, Monteville Formation. Cross Nicols. Scale bar—0.5 mm. For further explanation see Simonson (1992). Courtesy B.M. Simonson.

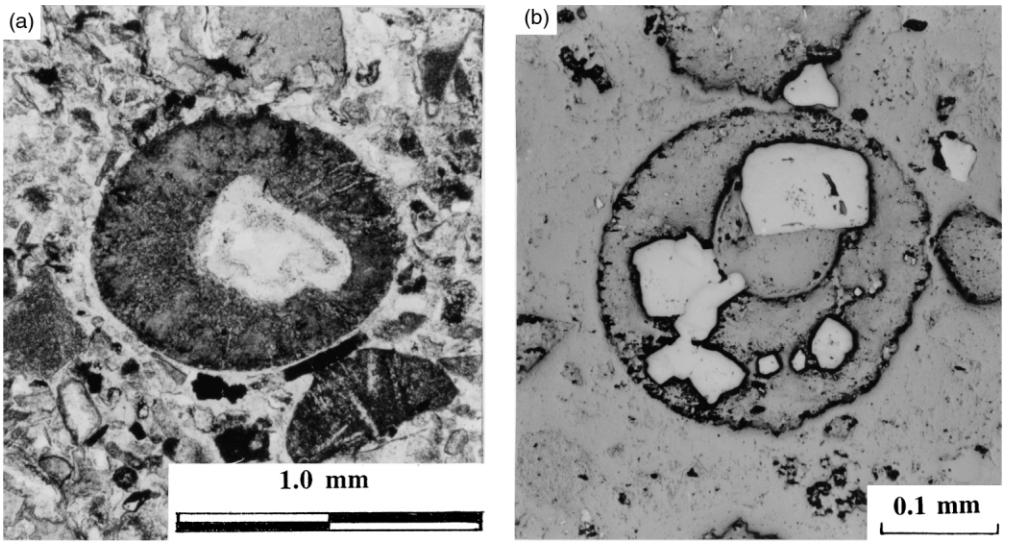

Plate 3. Impact spherules from the S3 spherule unit at the base of the 3.24 Ga Fig Tree Group (turbidites, felsic volcanics), Barberton Mountain Land, Transvaal. (a) Chlorite-dominated spherule showing an offset feldspar-filled gas bubble. The spherule is set in fine grained sandstone. Plane polarised light; (b) a reflected light microphotograph of an impact spherule from the S3 unit, with offset gas bubble, partly replaced by sulphide. Sample courtesy of G.R. Byerly. Photo by A.Y. Glikson.

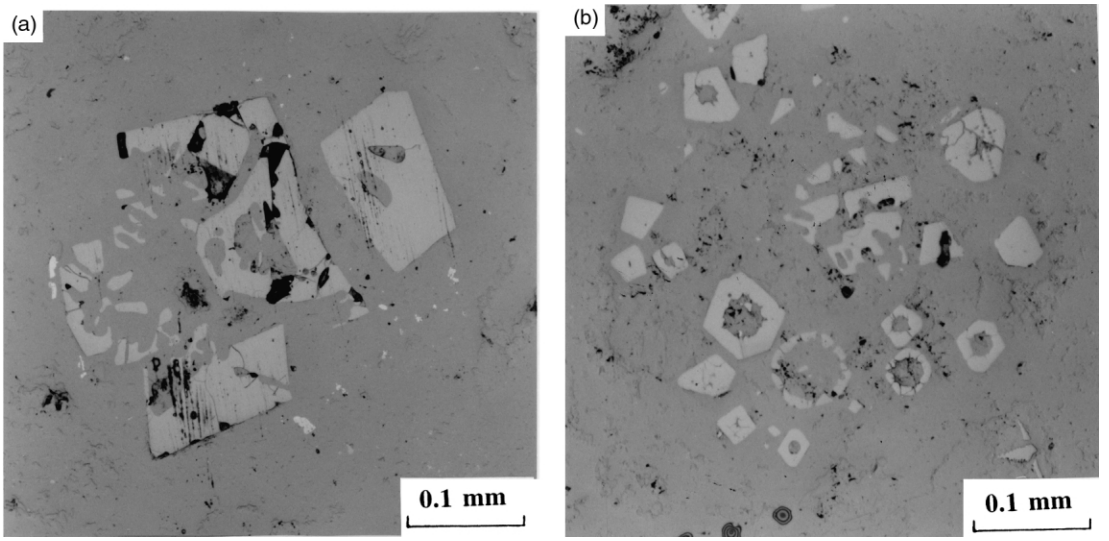

Plate 4. Resorbed Ni-rich chromites from spherules in the Fig Tree S3 unit. (a) A resorbed single Ni-rich chromite crystal. Note small sulphide grains at lower right; (b) a rosette of centrally resorbed chromites. Reflected light. Sample courtesy of G.R. Byerly. Photo by A.Y. Glikson.

Plate 5. A view of the eastern flank of the Steynsdorp anticline, Barberton Mountain Land, Transvaal, showing volcanics and interbedded cherts of the upper Onverwacht Group at low levels of the escarpment; turbidites of the Fig Tree Group forming steep smooth slopes at mid-level of the escarpment, and uppermost cliffs consisting of quartzite and conglomerate of the Moodies Group. The basal Fig Tree spherule units occur immediately above the fundamental break between the simatic 3.56–3.44 Ga Onverwacht Group and the turbidite-dominated c. 3.24 Ga Fig Tree Group (see arrow). Photo by A.Y. Glikson.

in Phanerozoic impact markers, including the K–T and E–O boundaries (Kyte and Smit, 1986) (Plate 1); (4) occurrence of PGE nuggets within the Ni-rich chromites (Taylor and Glikson, unpublished data, 2000); (5) uniquely extraterrestrial 53Cr/52Cr isotopic ratios in spherule unit S4 similar to C1 chondrites (Shukolayukov et al., 2000).

Koeberl et al. (1993) questioned the origin of the Barberton spherules on the basis of (1) alteration of PGE patterns associated with sulfide metasomatism, and (2) suggested derivation of the chromites by erosion of exposed nickel-rich intrusive ultramafic rocks of the Bon Accord type (Tredoux et al., 1989). However, a meteoritic impact connection of the spherules is supported by the following (Byerly and Lowe, 1994; Glikson, 1994): (1) the PGE patterns of the spherule-bearing sediments show depletion in the volatile and mobile species Pd and Au relative to the refractory Ir, a profile contrasted with the universal enrichment in the volatile PGE in both fresh and altered terrestrial rocks, excepting depleted harzburgites; (2) the extreme Ni values are unique to impact-condensation spherules: thus Ni values of chromites segregated by sulphide immiscibility (Grove et al., 1977; Czamanske et al, 1976) are more than one order of magnitude lower than those of the Barberton chromites; (3) derivation of the Ni-rich chromites by denudation of exposed equivalents of Ni-rich peridotites of the Bon Accord type (Tredoux et al., 1989) is equally unlikely, as Bon Accord chromites have lower Ni values, display enriched volatile PGE levels, and are unlikely to occur as quench skeletal crystals within spherules.

Lowe et al. (1989) and Lowe and Byerly (1990) remarked on the potential tectonic significance of the juxtaposition between the ~3.24 Ga impacts and the abrupt break between the underlying mafic-ultramafic volcanic environment (Onverwacht Group—3.55–3.24 Ga) and the overlying turbidite, felsic volcanic and conglomerate-dominated environment (Fig Tree and Moodies Groups), which includes the earliest observed granite-derived detritus (Plate 5). These relations may be interpreted in terms of onset of strong differential vertical movements triggered by

regional to global tectonic effects of the mega-impacts about 3.24 Ga, including rifting of the Onverwacht Group, strong uplift and formation of fault troughs within which the Fig Tree turbidites and felsic pyroclastics accumulated.

The period ~3.24 Ga is extensively represented in the western Pilbara (Sun and Hickman, 1998) and the central Pilbara Strelley-Soanesville belt (Van Kranendonk and Morant, 1998), where volcanics and cherts of the 3.26–3.24 Ga Sulphur Springs Group are unconformably overlain by a sequence of ferruginous siltstone and banded iron formation of the Gorge Creek Group. As in the Barberton, the latter contain granitoid detritus. To date, despite a recent search, no impact spherules have been found in these sequences.

Estimates of the scale of the projectiles, and thereby of consequent impact craters, are allowed by two different methods: (1) mass balance calculations based on abundances of Ir, Cr isotopes and other elements, assuming global distribution and mean thickness values based on field data (Lowe et al., 1989; Byerly and Lowe, 1994). For spherule unit S4—mass balance calculations indicate a chondritic projectile of >30 km-diameter; (2) spherule sizes, calibrated thermo-dynamically to the density of the vapour cloud from vapour-liquid phase boundary relations calibrated by Melosh and Vickery (1991) Spherules are commonly ~1–2 mm but can reach 4 mm in diameter, suggesting projectile diameters in the range of 20–50 km. Scaling of projectile/crater diameter relations by a factor of ~20 correspond to marescale craters 400–1000 km in diameter.

No shocked quartz fragments containing planar deformation lamella (PDF) were found with the Barberton spherule units. Because impacted sialic crust can be expected to contribute significant proportion of shocked quartz grains to the dust cloud, this absence militates for derivation from oceanic impact sites (Lowe et al., 1989), as is also the case with spherule units in the Hamersley Basin, Western Australia (Simonson, 1992; Simonson and Hassler, 1997) (Plate 2). The Barberton spherules thus provide information on large terrestrial impact basins located within Archaean oceanic crustal regimes.

6. Oceanic impacts and Precambrian magmatic-tectonic episodes

The dominance of simatic crustal regimes during the Precambrian requires special consideration of the effects of large oceanic impacts on crustal evolution (Roddy et al., 1987; Glikson, 1999). The formation of a 100 km-diameter crater can be modeled in terms of impact by a chondritic (3.0 g cm^{-3}) projectile of $Dp \sim 5$ km and a typical approach velocity of 24.6 km s^{-1} (Grieve, 1980). Penetration to a depth of 6–8 km (~1.5 Dp) and explosive energy release on the scale of $E >= 10^{22}$ Joules ($>10^6$ megatons TNT-equivalent) result in a transient crater with Dtc~ 50–60 km, followed by elastic rebound and expansion into a ring structure with a diameter of ~ 2Dtc (~20 Dp). The crustal column affected by the rebound (structural uplift, Su), observed as $Su = 0.086\ Dc^{1.03}$ (Grieve and Pilkington, 1996), will be ~10 km, resulting in ~3.3 kbar decompression of underlying mantle. Computer modeling by Roddy et al. (187) for impact by a $Dp = 10$ km asteroid indicates excavation of a transient oceanic crater with $Dc = 105$ km and a depth of dtc~27 km, followed by rebound effects through a depth similar to or greater than dtc. The extent of rebound-induced adiabatic melting in the mantle is related to the local geothermal gradient and to a lesser extent shock heating (Grieve, 1980). Excavation of the asthenosphere

may result in formation of magma lakes with volume in excess of crater dimensions, manifested by Large Igneous Provinces (LIP)-like situations (Grieve et al., 1999). A lower limit on the volume of affected crust and lithosphere approximates a vertical cylinder defined by *Su* and *Dc*. Impacts producing craters $Dc = 100$ km and $Dc = 300$ km will affect volumes of crust and lithosphere of about 9×10^5 km^3 and 2.2×10^6 km^3, respectively. For craters with $Dc = 300$ km and 10-50% mantle melting, volumes of produced magma range from 0.22×10^6 km^3 for basaltic magmas to 1.1×10^6 km^3 for peridotitic komatiite magma.

It is relevant to compare the volumes of modeled impact rebound-produced basalt relative to continental plateau basalts, oceanic large igneous provinces (LIPs), and Archaean mafic-ultramafic volcanism. Estimated volumes of continental basalts and their hypabyssal equivalents (Columbia Plateau: $\sim10^6$ km^3; North Atlantic volcanic province: $\sim7\times10^6$ km^3; Deccan traps: $\sim8\times10^6$ km^3) (Coffin and Eldholm, 1994) and minimum volumes of Archaean greenstones (ca. 3.47 Ga Warrawoona Group, Pilbara craton, Western Australia: $>0.25\times10^6$ km^3; ca. 2.7 Ga greenstones in the Eastern Goldfields, Western Australia: $>2\times10^6$ km^3), and the largest LIPs, i.e. Ontong-Java Plateau and Kerguelen Plateau, are similar to, or larger by an order of magnitude than, modeled volumes of impact-produced basalts for craters $>=300$ km in diameter.

Large impact events on thin (<5 km), geothermally active (>25 °C km^{-1}) oceanic crust overlying shallow asthenosphere (<40 km) may result in localization and/or accentuation of mantle convection cells and sea-floor spreading centers. Green (1981) suggested that Archaean peridotitic komatiites formed by $\sim50\%$ catastrophic melting upon lithospheric rebound, ascent of mantle diapirs, adiabatic melting, and intersection of the hydrous and dry pyrolite solidi at upper asthenospheric levels (Fig. 4). Under pressures of >60 kbar smaller degrees of melting can produce ultrabasic melts (C.G. Ballhaus, 1998, personal communication). Upon impact, propagation of radial lithospheric faults may result in migrating loci of mantle and crust melting. Where such faults intersect older greenstone–granitoid nuclei, magmatically active rifted zones ensue. This model is consistent with the multiple superposition of greenstone-granitoid cycles indicated above. Since impacted oceanic crust has been obliterated by burial, metamorphism and subduction, the only direct evidence may be provided by distal fallout deposits.

Under the high heat-flow levels prevailing in Archaean oceanic regimes, the basaltic crust would not transform into eclogite, placing constraints on the density-driven subduction model (Green, 1981). An alternative model involving impact-triggered episodic two-stage mantle melting processes (Glikson, 1993, 1996) includes: (1) large-scale melting of rebounding suboceanic asthenosphere; (2) gravitational collapse of thick slabs of oceanic crust dominated by high-density peridotite komatiite ($>14\%$ total iron as FeO; ~3.4 g.cm^{-3}) into underlying olivine-dominated lower density asthenosphere (~3.3 g.cm^{-3}); and (3) long-term geothermal rises associated with cratered aureoles result in second-stage melting of the ultramafic-mafic crust, producing dacitic magmas.

7. The impact factor and Mesozoic–Cainozoic plate tectonics patterns

Alt et al. (1988) and Oberbeck et al. (1992) developed an elaborate case for impact-triggered continental volcanism and rift-splitting of Gondwana as a principal factor underlying spatial Mesozoic–Cainozoic plate tectonic patterns. The global seismic consequences of mega-impacts (Hughs et al., 1977; Boslough et al., 1994) and impact-triggered lithospehric faults (Jones, 1987)

provide possible explanations for these models. Some potential but unproven impact-tectonic connections are listed in Table 2, including (1) Cretaceous–Tertiary boundary (ca. 65 Ma) impact(s), onset of the Carlsberg Ridge Indian Ocean spreading, Deccan volcanism, and onset of the mantle plume of the Emperor–Hawaii chain; (2) Jurassic–Cretaceous boundary (ca. 141 Ma) impacts (Morokweng, Gosses Bluff, Mjolnir), onset of Gondwana breakup, including initiation of the Mesozoic precursor of the Syrian-African rift system.; (3) late Triassic (~205 Ma) impacts (Manicouagan, Saint Martin, Puchezh-Katunki), opening of the south-central Atlantic Ocean and widespread rifting, extensive rifting and alkali volcanic activity; (4) Permian–Triassic boundary (~251 Ma) impact(s) [Araguainha impact, Brazil (Bischoff and Prinz, 1994)], shocked quartz in Permian–Triassic boundary sediments (Rettalack et al., 1998), the Siberian Norilsk volcanic traps (248±2.4 Ma) and early Triassic rifting. However, due to the nature of the circumstantial evidence, definitive criteria are required to test such potential correlations.

Phanerozoic Apparant Pole Wander Paths (APWP) display sharp trend changes (loops and cusps) which in some instances approximately coincide with impact clusters. Loops documented by Klootwijk (1996) from Australian APWPs include: (1) 300 Ma loop (Carboniferous–Permian boundary); (2) 280–270 Ma loop; (3) 260 Ma loop; (4) 250 Ma cusp; (5) 140 Ma loop; (6) 100–115

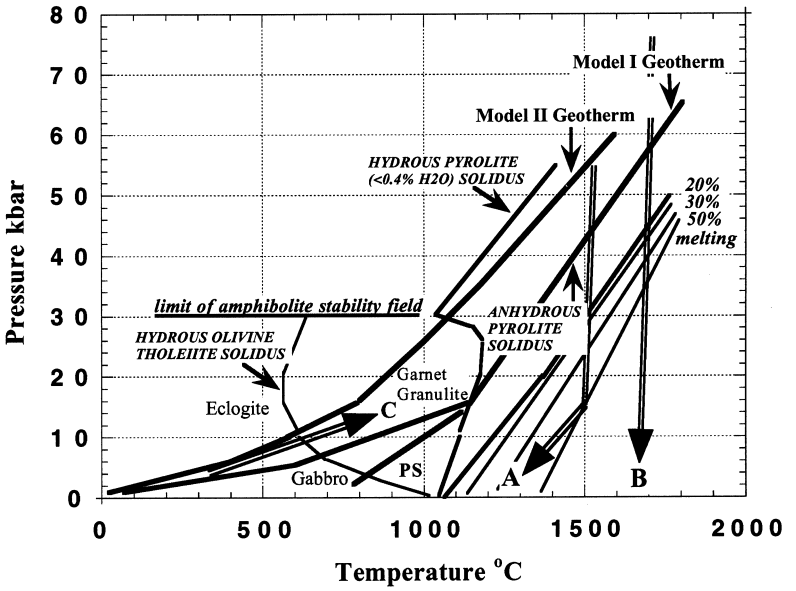

Fig. 4. Pressure-temperature plot of oceanic geothermal regimes, metamorphic P-T fields, hydrous and anhydrous solidi of mantle and crust materials, and percent melting curves for anhydrous mantle (after Green, 1981). PS- superposed postshock heat effects (after Grieve, 1980). Boundaries show anhydrous pyrolite solidus, hydrous pyrolite solidus, amphibole breakdown curve, basalt melting curve, and hydrous basalt melting curve. Model geotherms: Model I—oceanic geotherm (~25 °C km^{-1}); model II—continental geotherm (~12 °C km^{-1}). Arrows: A—rebound P–T transport path of mantle excavated by 100-km-diameter crater with central uplift of 10 km; B—rebound P–T transport path of mantle excavated by 300 km-diameter crater with central uplift of 30 km; C—subsidence and partial melting P–T transport path of high density komatiite-dominated mafic crust collapsed into olivine-dominated residual mantle.

Table 2
Listing of near contemporaneous impact structures, volcanic and tectonic events. No genetic relationship is necessarily implied. Data for impact structures after Grieve (1997) crater@gsc.nrcan.gc.ca

Impact structure and fallout	*Dc*	Age	Volcanic/tectonic activity and palaeomagnetic signatures	Age (Ma)
Chesapeake Bay	85	35.5±0.6	Ethiopian Plateau basalts	35±2
Popigai	100	35.5±0.8		
Chicxulub	170	64.98±0.05	Deccan Plateau basalts;	~65
? Shiva structure (sub-Deccan Plateau basalts)			Carlsberg Ridge; Emperor-Hawaii chain	
Morokweng	90	145±0.8	Period of southern Gondwanaland breakdown	
Mjolnir	40	143±20		
Gosses Bluff	24	142.5±0.8		
Manicouagan	100	214±1	Atlantic split and global rifting, extensive rifting and mafic volcanism	
Saint Martin	40	220±32		
Rochechouart	23	214±8		
Obolon	15	215±25		
Red Wing	9	200±25		
Araguinha	40	247±5.5	Siberian Norilsk traps	248.3±0.3
PDF in quartz in sediments				

Ma cusp; (7) 70 Ma cust; (8) 45–40 Ma cusp. The poor age definition of these crustal motions does not allow potential correlations with dated impact events.

Criteria for identification of proposed impact-triggered faults, rift structures, mega-breccia and distal igneous activity remain little defined. For example, distinctions between possible impact breccia and glacial tillites remain to be clarified (Oberbeck et al., 1992; Rampino and Caldeira, 1993). The meagre number of precisely dated impact events, contrasted with the extensive body of isotopic ages of magmatic events, results in a strongly skewed database, disallowing statistical tests of significant correlations. On the other hand, the terrestrial impact flux considered above, coupled with the episodic nature of major magmatic events (Condie, 1995; Glikson, 1993, 1996), may hint at a possible relationship.

Impact-triggering of continental rifting and flood basalt (CFB) volcanism is not generally favoured by volcanologists, who mostly interpret the data in purely endogenic terms. Courtillot et al. (1999), on the basis of studies in the Red Sea-Gulf of Eden-Afar Triangle plate junction, suggest rapid upwelling of mantle plume beneath central parts of continental shields as the triggers of flood basalt, rifting, and ocean ridge spreading, consistent with Morgan (1981) and Hill (1991). The model accounts for a range of structural patterns, from active and hot rift zones which overlie plumes to passive cold peripheral rift branches, including spreading of the north, central, and south Atlantic Ocean, Indian Ocean, and the Arabian Sea.

Key observations regarding the origin of continental breakup are the large volume and high rate of extrusion of the CFB, involving volumes in the range of $0.5–8.0\times10^6$ km^3 emplaced at rate

of 1–8 km^3 $year^{-1}$—the maximum rate observed for the Deccan traps leads Courtillot et al. (1999) to the concept of "plume impact". Even greater volumes and similar to higher extrusion rates pertain in large oceanic igneous provinces (LIP), for example Ontong-Java Plateau ($3.6–5.5\times10^7$ km^3 over $<3\times10^6$ years, i.e. ~10–20 $km^3 year^{-1}$) and the Kerguelen Plateau ($1.6–2.4\times10^7$ km^3 over 4.5×10^6 years, i.e. ~3.5–5.0 km^3 $year^{-1}$) (Coffin and Eldholm, 1994). The violent short-lived nature of these volcanic episodes, as well as their location beneath both continental and oceanic crust, hints at yet unexplained triggering factor/s.

It is not clear how models of plume-triggered ocean basins are reconciled with the petrological and geochemical distinctions between Mid-ocean ridge basalts and plume alkaline basalts, traditionally interpreted in terms of derivation from shallow and deep levels of the asthenosphere, respectively (Richards et al., 1989; Griffith and Campbell, 1991). By contrast, Anderson (1998) suggested passive splitting of continental crust along early sutures and craton boundaries, reactivating melting within a near-solidus or above-solidus asthenosphere. The model is consistent with the common, although by no means universal, superposition of faulted African and Australian continental margins on older circum-cratonic Proterozoic sutures and mobile belts (Clifford, 1970).

Progress in the documentation and isotopic ages of volcanic provinces (Renne and Basu, 1991; Renne et al., 1996), as well as further deciphering of the terrestrial impact record (Grieve and Shoemaker, 1994; Shoemaker and Shoemaker, 1996; French, 1998), require a re-examination of the possibility of impact-triggered plate tectonic motions. The post-LHB impact rate within the inner solar system for craters larger than 20 km-diameter, considered above, implies formation during the Mesozoic-Cainozoic of about 30 craters with $Dc >= 100$ km and about 3 craters with $Dc >= 300$ km. Assuming a time-integrated 1:2 ratio of continental/oceanic crustal surfaces during the last 250×10^6 years, the minimum number of oceanic craters with $Dc >= 80$ km-diameter is defined by the 6 observed impact structures of $Dc >= 80$ km documented on the continents (Popigai—100 km, 35.7 ± 0.8 Ma; Chesapeake Bay—90 km, 35.2 Ma; Chicxulub—170 km, 64.98 Ma; Morokweng—90 km, 145 ± 3 Ma; Manicouagan—100 km, 214 ± 1 Ma; Puchezh-Katunki—80 km, $220\pm$ 10 Ma; Woodleigh—120 km, 364 ± 8) (data after Grieve, 1997; Mory et al., 2000; T. Uysal, personal communication, 2000). From the above, a minimum number of 11 oceanic craters of diameter $>= 80$ km is expected to have formed during the Mesozoic and Cainozoic, confirming over 50% of the 20 oceanic craters of $Dc >= 100$ km-diameter predicted by the lunar impact flux and present-day astronomical observations.

What are the signatures for these oceanic craters? What were the global seismic and magmatic effects of impacts impinging on mid-ocean spreading ridge environments? Could such distal effects of oceanic mega-impacts have reactivated old cratonic sutures according to Anderson's (1998) model? Few attempts at seismic and thermodynamic modelling of the distal/global consequences of mega-impacts have been reported to date (Hughs et al., 1977; Boslough et al., 1994). According to the latter, due to distal seismic refraction and focussing effects, no geographic proximity is necessarily expected between impact sites, faulting, rifting and volcanism. Could some of these impacts have triggered LIP provinces, and could the latter have flooded buried oceanic craters? Ockham's Razor principle requires that, where established factors or mechanisms are potentially capable of resolving a question, they should be considered at least as seriously as unknown mechanisms: whereas the existence of asteroid/comet mega-impacts is an established fact, the concept of "plume impact" (Courtillot et al., 1999) remains purely a model!

8. Concluding statement

The combination of evidence provided by the 3.24–3.227 Ga Barberton impact spherule units (Lowe and Byerly, 1986; Lowe et al., 1989; Byerly and Lowe, 1994; Shukolyukov et al., 2000), the lunar impact spherule evidence (Muller, 1993; Culler et al., 2000) (Fig. 5A), and the distribution of isotopic Rb-Sr ages (Fig. 5B) and Ar–Ar ages (Fig. 5C) of lunar mare basalts, constitutes the first well documented case for an Archaean impact cataclysm in the Earth–Moon system, with profound tectonic and magmatic consequences.

Much of the Archaean crustal record remains shrouded in mystery, not least the nature of the simatic crust which occupied over some 80% of the Earth. Compilations of Precambrian isotopic data have been interpreted in terms of continuous crustal accretion, distinct thermal and tectonic episodes (Condie, 1995; Glikson, 1993, 1996), or combined episodicity and accretion (Card, 1990). A global nature of these episodes is suggested by correlations between peak periods of thermal events in separate Precambrian shields. However, the significance of age-distribution

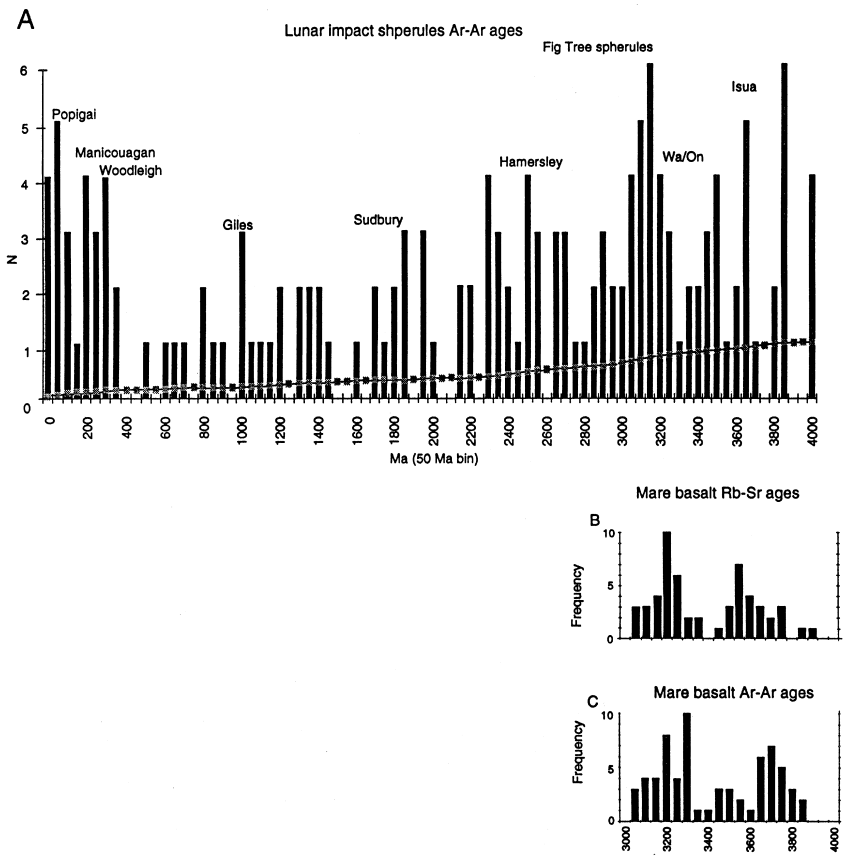

Fig. 5. (A) Frequency distribution of Ar–Ar ages of lunar impact spherules based on data by Culler et al. (2000), compared with (B) frequency distribution of Rb–Sr isotopic ages of mare basalts and (C) frequency distribution of Ar–Ar isotopic ages of mare basalts (C) (after Basaltic Volcanism of the Terrestrial Planets 1981). The ages of major terrestrial impact events are marked in diagram (A).

histograms is fraught with uncertainties arising from the likely selective preservation of crustal segments and from sampling bias due to economic and scientific priorities and terrain accessibility. The tentative episodic nature of mafic igneous activity suggested by age distribution diagrams may be interpreted in terms of purely endogenic factors, effects of mega-impacts (Glikson, 1993, 1996), or a combination of both. The role of large impacts in crustal evolution will be identified by their distal signatures- spherulitic melt condensates (microkrystites), microtektites, platinum group element anomalies, shocked quartz and zircon, distal ejecta, earthquake-generated rip-up clasts, and tsunami deposits. As pointed out by Marvin (1990), Hamilton (1998) and Anderson (1998), the history of Earth science constitutes a poignant warning against "science by consensus" notions. Projections of actualistic plate tectonic processes, which by their nature constitute uniformitarian assumptions rather than factual observations, can hardly replace analysis of the field data based on their own merits. The projection of sequence stratigraphy schemes into the Archaean (Krapez, 1993) may result in imposition of uniformitarian assumptions on very different and as yet little understood Earth, and may obscure the building blocks on which the history of Archaean greenstone belts needs to be built. Okcham's Razor parsimony rule, which requires that no unnecessary unknown factors are invoked in the interpretation of data, needs to be more closely respected in most Archaean models. The rocks must be allowed to speak for themselves.

Acknowledgements

I thank Wolf Jacoby for inviting me to prepare this review and Bruce Simonson and an anonymous referee for constructive comments. I thank Andreas Abels, Marco Andreoli, Chris Ballhaus, Vickie Bennett, Geoff Davies, Steve Drury, Warren Hamilton, Malcolm McCulloch, and Mike Palin for discussion of the issues considered in this paper.

References

Alt, A.D., Sears, J.W., Hyndman, D.W., 1988. Terrestrial maria: the origins of large basalt plateaus, hotspot tracks and spreading ridges. Journal Geology 96, 647–662.

Anderson, D.L., 1998. The edges of the mantle. In: Gurnis, M., Wysensson, M.E., Knittle, E., Buffett, B.A. (Eds.), The Core-Mantle Boundary Region, Geodynamics, Vol. 28. American Geophysical Union, Washington DC, pp. 255–271.

Anhaeusser, C.R., 1973. The evolution of the early Precambrian crust of southern Africa. Philosophical Transactions Geological Society London A273, 359–388.

Archibald, N.J., Bettenay, L.F., 1977. Indirect evidence for tectonic reactivation of pre-greesntone basement in Western Australia. Earth Planetary Science Letters 33, 370–378.

Arth, G.J., Hanson, G.N., 1975. Geochemistry and origin of the early Precambrian crust of northeastern Minnesota. Geochimica et Cosmochimica Acta 39, 325–362.

Ayres, L.D., 1974. Geology of the Trouts Lake area. Ontario Department Geology Mineral Report 113.

Baldwin, R.B., 1985. Relative and absolute ages of individual craters and the rates of infalls on the Moon in the post-Imbrium period. Icarus 61, 63–91.

Baragar, W.R.A., Goodwin, A.M., 1969. Andesites and Archaean volcanism in the Canadian Shield. Oregon Department Geology Mineral Industry Bulletin 65, 121–141.

Baragar, W.R.A., McGlynn, J.C., 1976. Early Archaean basement in the Canadian Shield: a review of the evidence. Geological Survey Canada Special Paper 76–14.

Barley, M.E., 1993. Volcanic, sedimentarty and tectonostratigraphic environments of the ~3.46 Ga Warrawoona megasequence: a review. Precambrian Research 60, 47–67.

Barlow, N.G., 1990. Estimating the terrestrial crater production rate during the late heavy bombardment period. Lunar and Planetary Institute Contribution 746, 4–7.

Basaltic Volcanism of the Terrestrial Planets, 1981. Pergamon, New York.

Binns, R.A., Gunthorpe, R.J., Groves, D.I., 1976. Metamorphic patterns and development of greenstone belts in the eastern Yilgarn Block, Western Australia. In: Windley, B.F. (Ed.), Early History of the Earth. John Wiley & Sons, London, pp. 331–350.

Bischoff, L., Prinz, T., 1994. Der Araguinha-Krater in Brasilien. Geowissenschaften 12, 354–360.

Boslough, M.B., Chael, E.P., Trucano, T.G., Kipp, M.E., Crawford, D.A., 1994. Axial focussing of impact energy in the Earth's interior: proof-of-principle tests of a new hypothesis. Lunar Planetary Institution Contribution 825, 14–15.

Bridgwater, D., Collerson, K.D., 1976. The major petrological and geochemical characters of the 3600 m.y. Uivak gneisses from Labrador. Contributions Mineralogy Petrology 54, 43–56.

Byerly, G.R., Lowe, D.R., 1994. Spinels from Archaean impact spherules. Geochimica et Cosmochimica Acta 58, 3469–3486.

Byerly, G.R., Kroner, A., Lowe, D.R., Todt, W., Walsh, M.M., 1995. Prolonged magmatism and time constraints for sediment deposition in the early Archaean Barberton greenstone belt: evidence from the Upper Onverwacht and Fig Tree groups. Precambrian Research 78, 125–138.

Campbell, I.H., Griffiths, R.W., 1992. The changing nature of mantle hot spots through time: implications for the chemical evolution of the mantle. Journal of Geology 92, 497–523.

Card, K.D., 1990. A review of the Superior Province of the Canadian Shield—a product of Archaean accretion. Precambrian Research 48, 99–156.

Chadwick, B., Ramakrishnan, M., Viswanatha, M.N., Murthy, V.S., 1978. Structural studies in the Archaean Sargur and Dharwar supracrustal rocks of the Karnataka Craton. Journal Geological Society of India 29, 531–542.

Clifford, T.N., 1970. The structural framework of Africa. In: Clifford, T.N., Gass, I.G. (Eds.), African Magmatism and Tectonics. Oliver and Boyd, Edinburgh, pp. 1–26.

Coffin, M.F., Eldholm, O., 1994. Large igneous provinces: crustal structure, dimensions and external consequences. Review of Geophysics 32, 1–36.

Compston, W., Williams, I.S., Campbell, I.H., Gresham, J.J., 1986. Zircon xenocrysts from the Kambalda volcanics: age constraints and direct evidence of an older continental crust below the Kambalda-Norseman greenstones. Earth Planetary Science Letters 76, 299–311.

Condie, K.C., 1995. Episodic ages of greenstone: a key to mantle dynamics? Geophysical Research Letters 22, 2215–2218.

Corner, B., Reimold, W.U., Brandt, D., Koeberl, C., 1997. Morokweng impact structure, Northwest province, South Africa: geophysical imaging and shock petrographic studies. Earth Planetary Research Letters 146, 351–364.

Courtillot, V., Jaupart, C., Manughetti, I., Tapponnier, P., Besse, J., 1999. On causal links between flood basalts and continental breakup. Earth Planetary Research Letters 166, 177–196.

Czamanske, G.K., Himmelberg, G.R., Goff, F.E., 1976. Zoned Cr-Fe-spinels from the La Perouse layered gabbro, Fairweather Range, Alaska. Earth Planetary Research Letters 33, 111–118.

Culler, T.S., Becker, T.A., Muller, R.A., Renne, P.R., 2000. Lunar impact history from 39Ar/40Ar dating of glass spherules. Science 287, 1785–1789.

de Wit, M.J., Hart, R.A., Hart, R.J., 1987. The Jamestown ophiolite complex, Barberton Mountain belt: a section through 3.5 Ga oceanic crust. Journal African Earth Science 6, 681–730.

de Wit, M.J., 1982. Gliding and overthrust nappe tectonics in the Barberton greenstone belt. Journal Structural Geology 4, 117–136.

de Wit, M.J., 1998. On Archaean granites, greenstones, cratons and tectonics: does the evidence demand a verdict? Precambrian Research 91, 181–226.

Deutsch, A., 1998. Examples for terrestrial impact structures. In: Marfunin, A.S. (Ed.), Advanced Mineralogy. Springer-Verlag, Berlin, pp. 119–129.

Donaldson, J.A., Jackson, G.D., 1965. Archaean sedimentary rocks of north Spirit Lake area, northwestern Ontrio. Canadian Journal Earth Science 2, 622–647.
Drury, S., 1999. Stepping Stones—The Making of our Home World. Oxford University Press, Oxford.
Engel, A.E.J., 1966. The Barberton Mountain Land: clues to the differentiation of the Earth. University of Witwatersrand Information Circular 27, Johannesburg.
Folinsbee, R.E., Baadsgaard, H., Cumming, G.L., Green, D.C., 1968. A very ancient island arc. American Geophysical Union Monograph 12, 441–448.
French, B.M., 1998. Traces of Catastrophe. Lunar Planetary Science Contributions 954.
Gee, R.D., 1976. Regional geology of the Archaean nuclei of the Western Australian Shield. In: Knight, L. (Ed.), Economic Geology of Australia and Papua New Guinea. Australia Institute Mining Metallurgy, Melbourne, pp. 66–74.
Glikson, A.Y., 1970. Geosynclinal evolution and geochemical affinities of early Precambrian systems. Tectonophysics 9, 397–433.
Glikson, A.Y., 1971. Primitive Archaean element distribution patterns: chemical evidence and tectonic significance. Earth Planetary Science Letters 12, 309–320.
Glikson, A.Y., 1972. Early Precambrian evidence of a primitive ocean crust and island nuclei of sodic granite. Geological Society America Bulletin 83, 3323–3344.
Glikson, A.Y., 1980. Uniformitarian assumptions, plate tectonics and the Precambrian Earth. In: Kroner, A. (Ed.), Precambrian Plate Tectonics. Elsevier, Amsterdam, pp. 91–104.
Glikson, A.Y., 1983. Geochemical, isotopic and palaeomagnetic tests of early sial-sima patterns: the Precambrian crustal enigma revisited. Geological Society America Memoir 4, 183–219.
Glikson, A.Y., 1984. Significance of early Archaean mafic- ultramafic xenolith patterns. In: Kroner, A., Goodwin, A.M., Hanson, G.N. (Eds.), Archaean Geochemistry. Springer-Verlag, Berlin, pp. 263–280.
Glikson, A.Y., 1993. Asteroids and early Precambrian crustal evolution. Earth Science Reviews 35, 285–319.
Glikson, A.Y., 1994. Archaean spherule beds: impact or terrestrial origin? Earth Planetary Science Letters 26, 493–496.
Glikson, A.Y., 1996. Mega-impacts and mantle melting episodes: tests of possible correlations. Australian Geological Survey Organisation Journal Australia Geology and Geophysics 16, 587–608.
Glikson, A.Y., 1999. Oceanic mega-impacts and crustal evolution. Geology 27, 341–387.
Glikson, A.Y., Sheraton, J.W., 1972. Early Precambrian trondhjemitic suites in Western Australia and northwestern Scotland and the geochemical evolution of shields. Earth Planetary Science Letters 17, 227–242.
Glikson, A.Y., Lambert, I.B., 1976. Vertical zonation and petrogenesis of the early Precambrian crust in Western Australia. Tectonophysics 30, 55–89.
Glikson, A.Y., Ballhaus, C.G., Clarke, G.C., Sheraton, J.W., Sun, S.S., 1995. Geology of the Giles Complex and Environs, western Musgrave Block, central Australia. Australian Geological Survey Organisation Bulletin 239, 209.
Gorter, J.D., 1998. The petroleum potential of Australian Phanerozoic impact structures. Australian Petroleum Exploration Journal 37, 159–186.
Green, D.H., 1972. Archaean greenstone belts may include terrestrial equivalents of lunar maria? Earth Planetary Science Letters 15, 263–270.
Green, D.H., 1981. Petrogenesis of Archaean ultramafic magmas and implications for Archaean tectonics. In: Kroner, A. (Ed.), Precambrian Plate Tectonics. Elsevier, Amsterdam, pp. 469–489.
Grieve, R.A.F., 1980. Impact bombardment and its role in proto-continental growth of the early Earth. Precambrian Research 10, 217–248.
Grieve, R.A.F., 1997. Impact crater database—crater@gsc.nrcan.gc.ca.
Grieve, R.A.F., Dence, M.R., 1979. The terrestrial cratering record: II. The crater production rate. Icarus 38, 230–242.
Grieve, R.A.F., Shoemaker, E.M., 1994. The Record of Past Impacts on Earth. The University of Arizona Press, Tucson, Arizona.
Grieve, R.A.F., Pesonen, L.J., 1996. Terrestrial impact craters: their spatial and temporal distribution and impacting bodies. Earth, Moon and Planets 72, 357–376.
Grieve, R.A.F., Pilkington, M., 1996. The signature of terrestrial impacts. Australian Geological Survey organisation Journal Australian Geology and Geophysics 16, 399–420.
Grieve, R.A.F., Cintala, M.J., Therriault, A.M., 1999. Impact basins and crustal evolution (abstract). International Symposium Planetary Impact Events and their Consequences on Earth, Yamaguchi, Japan, p. 33.

Griffiths, R.W., Campbel, I.H., 1991. Interaction of mantle plume heads with the Earth's surface and onset of small scale convection. Journal Geophysical Research 96, 18295–18310.
Grove, D.I., Barrett, F.M., Binns, R.A., McQueen, K.G., 1977. Spinel phases associated with metamorphosed volcanic-type iron-nickel sulphide ores from Western Australia. Economic Geology 72, 1224–1244.
Gruau, G., Jahn, B., Glikson, A.Y., Davy, R., Hickman, A.H., Chauvel, C., 1987. Age of the Archaean Talga-Talga Subgroup, Pilbara Block, Western Australia, and early evolution of the mantle: new Sm-Nd evidence. Earth Planetary Science Letters 85, 105–116.
Hamilton, W.B., 1998. Archaean magmatism and deformation were not products of plate tectonics. Precambrian Research 91, 143–179.
Henderson, J.B., 1975. Sedimentological studies in the Yellowknife Supergroup, District of MacKenzie. Geological Survey Canada Paper 70-26.
Hickman, A.J., 1981. Crustal evolution of the Pilbara Block, Western Australia. Geological Society Australia Special Publication 7, 57–69.
Hietanen, A., 1975. Generation of potassium-poor magmas in the northern Sierra Nevada and the Svecofennian of Finland. United States Geological Survey Journal Research 3, 631–645.
Hill, R.I., 1991. Starting plumes and continental breakup. Earth Planetary Science Letters 104, 398–416.
Hughs, H.G., App, F.N., McGetchin, T.N., 1977. Global seismic effects of basin-forming impacts. Physics of the Earth and Planetary Interiors 15, 251–263.
Hunter, D.R., 1970. The ancient gneiss complex in Swaziland. Transactions Geological Society Africa 73, 105–107.
Hunter, D.R., 1974. Crustal development in the Kaapvaal Craton: part 1—the Archaean. Precambrian Research 1, 259–294.
Jahn, B.M., Glikson, A.Y., Peucat, J.J., Hickman, A.H., 1980. REE geochemistry and geochronology of Archaean silicic volcanics and granitoids from the Pilbara Block, Western Australia. Geochimica et Cosmochimica Acta 45, 1633–1652.
Jones, A.G., 1987. Are impact-generated lower crustal faults observable? Earth Planetary Science Letters 85, 248–252.
Kamo, S.L., Davis, D.W., 1994. Reassessment of Archaean crustal development in the Barberton Mountain Land, South Africa, based on U-Pb dating. Tectonics 13, 167–192.
Klootwijk, C., 1996. Phanerozoic configurations of Greater Australia: evolution of the Northwest shelf. Australian Geological Survey Organisation Record 1996, 52.
Koeberl, C., Reimold, W.U., Boer, R.H., 1993. Geochemistry and mineralogy of early Archaean spherule beds, Barberton Mountain Land, South Africa: evidence for origin by impact doubtful. Earth Planetary Science Letters 119, 441–452.
Krapez, B., 1993. Sequence stratigraphy of the Archaean supracrustal belts of the Pilbara Block, Western Australia. Precambrian Research 60, 1–45.
Kroner, A., 1981. Precambrian plate tectonics. In: Kroner, A. (Ed.), Precambrian Plate Tectonics. Elsevier, Amsterdam, pp. 469–489.
Kroner, A., Hegner, E., Wendt, J.I., Byerly, G.R., 1996. The oldest part of the Barberton granitoid-greenstone terrain, South Africa: evidence for crust formation between 3.5–3.7 Ga. Precambrian Research 78, 105–124.
Kyte, F.T., Smit, J., 1986. Regional variations in spinel compositions: an important key to the Cretaceous/Tertiary event. Geology 14, 485–487.
Kyte, F.T., Zhou, L., Lowe, D.R., 1992. Noble metal abundances in an early Archaean impact deposit. Geochimica et Cosmochimica Acta 56, 1365–1372.
Lambert, R.St.J., 1975. Archaean thermal regimes, crustal and upper mantle temperatures, and a progressive evolutionary model for the Earth. In: Windley, B.F. (Ed.), The Early History of the Earth. John Wiley & Sons, London, pp. 363–376.
Lowe, D.R., Byerly, G.R., 1986. Early Archaean silicate spherules of probable impact origin, South Africa and Western Australia. Geology 14, 83–86.
Lowe, D.R., Byerly, G.R., 1990. Tectonic and sedimentological effects of large 3250 million years old meteorite impacts, Barberton greenstone belt. Abstracts Annual Meeting Geological Society America.
Lowe, D.R., Byerly, G.R., Asaro, F., Kyte, F.T., 1989. Geological and geochemical record of 3400 Million years old terrestrial meteorite impacts. Science 245, 959–962.

Marvin, U.B., 1990. Impact and its revolutionary implications for geology. Geological Society of America Special Paper 247, 147–154.
McCulloch, M.T., Bennett, V.C., 1994. Progressive growth of the Earth's continental crust and depleted mantle: geochemical constraints. Geochimica et Cosmochimica Acta 58, 4717–4738.
Melosh, H.J., Vickery, A.M., 1991. Melt droplet formation in energetic impact events. Nature 350, 494–497.
Morgan, W.J., 1981. Hotspot tracks and the opening of the Atlantic and Indian oceans. In: Emiliani, C. (Ed.), The Sea, Vol. 7. Wiley Interscience, New York, pp. 443–487.
Mory, A.J., Iasky, R.P., Glikson, A.Y., Pirajno, F., 2000. Woodleigh—a new 120 km impact structure, Carnarvon Basin, Western Australia. Earth Planetary Science Letters 177, 119–128.
Muller, R.A., 1993. Technical Report LBL-34168, Lawrence Berkeley National Laboratory, Berkeley, CA.
Myers, J.S., 1995. The generation and assembly of an Archaean supercontinents: evidence from the Yilgarn craton, Western Australia. Geological Society London Special Publication 95, 1439–1454.
Naqvi, S.M., 1976. Physical-chemical conditions during the Archaean as indicated by Dharwar geochemistry. In: Windley, B.F. (Ed.), Early Hisitory of the Earth. John Wiley & Sons, London, pp. 289–298.
Oberbeck, V.R., Marshall, J.R., Aggarval, H., 1992. Impacts, tillites and the breakdown of Gondwanaland. Journal Geology 101, 1–19.
Oversby, V.M., 1975. Lead isotopic systematics and ages of Archaean acid intrusives in the Kalgoorlie-Norseman area, Western Australia. Geochimica et Cosmochimica Acta 40, 1107–1125.
Padgham, W.A., 1992. The Slave structural province, North America: a discussion of tectonic models. In: Glover, J.E., Ho, S.E. (Eds.), The Archaean Terrains, Processes and Metallogeny, Vol. 22. University Western Australia Publication, pp. 381–394.
Pesonen, L.J., 1996. The impact cratering record of Fennoscandia. Earth, Moon, and Planets 72, 377–393.
Ramakrishnan, M., Wiswanatha, M.N., Swami Nath, J., 1976. Basement-cover relationships of Peninuslar gneiss with high grade schists and greenstone belts of southern Karnataka. Journal Geological Society India 17, 97–111.
Rampino, M.R., Caldeira, K., 1993. Major episodes of geologic change: correlation, time structure and possible causes. Earth Planetary Science Letters 114, 215–227.
Rennes, P., Basu, A.R., 1991. Rapid eruption of the Siberian traps flood basalts at the Permian-Triassic boundary. Science 253, 176–179.
Rennes, P., Deckart, K., Ernesto, M., Feraud, G., Picrillo, E.M., 1996. Age of the Ponta Grossa dike swarm (Brazil), and implications to Parana flood volcanism. Earth Planetary Science Letters 144, 199–211.
Rettalack, G.J., Seyedolali, A., Krull, E.S., Holser, W.T., Ambers, C.P., Kyte, F.T., 1998. Search for evidence on impact at the Permian-Triassic boundary in Antarctica and Australia. Geology 26, 979–982.
Richards, M.A., Duncan, R.A., Courtillot, V., 1989. Flood basalts and hot spot tracks: plume heads and tails. Science 246, 103–107.
Roddy, D.J., Schuster, S.H., Rosenblatt, M., Grant, L.B., Hassig, P.J., Kreyenhagen, K.N., 1987. Computer simulation of large asteroid impacts into oceanic and continental sites—preliminary results on atmospheric, cratering and ejecta dynamics. International Journal Impact Engineering 5, 525–541.
Ryder, G., 1990. Lunar samples, lunar accretion and the early bombardment of the Moon. Eos 71, 313–322.
Ryder, G., 1991. Accretion and bombardment in the Earth-Moon system: the Lunar record. Lunar Planetary Institute Contribution 746, 42–43.
Ryder, G., 1997. Coincidence in the time of the Imbrium Basin impact and Apollo 15 Kreep volcanic series: impact-induced melting? Lunar Planetary Institute Contribution 790, 61–62.
Shoemaker, E.M., Shoemaker, C.S., 1996. The Proterozoic impact record of Australia. Australian Geological Survey Organisation Journal Australia Geology Geophysics 16, 379–398.
Shukolyukov, A., Kyte, F.T., Lugmair, G.W., Byerly, G.R., 2000. The oldest impact deposits on Earth. In: Proceeding Conference on Impacts and the Early Earth, Cambridge, UK, December 1998.
Simonson, B.M., 1992. Geological evidence for an early Precambrian microtektite strewn field in the Hamersley Basin of Western Australia. Geological Society America Bulletin 104, 829–839.
Simonson, B.M., Hassler, S.W., 1997. Revised correlations in the early Precambrian Hamersley Basin based on a horizon of resedimented impact spherules. Australian Journal Earth Science 44, 37–48.
Sun, S.S., Hickman, A.H., 1998. New Nd-isotope and geochemical data from the west Pilbara—implications for

Archaean crustal accretion and shear zone movement. Australian Geological Survey Organisation Research Newsletter 28, 25–28.
Sutton, J., 1971. Some developments in the crust. Geological Society Australia Special Publication 3, 1–10.
Tarney, J., Dalziel, I.W.D., de Wit, M.J., 1976. Marginal Basin 'Rocas Verdes' complex from south Chile: a model for Archaean greenstone belt formation. In: Windley, B.F. (Ed.), The Early History of the Earth. John Wiley & Sons, New York, pp. 131–146.
Tredoux, M., de Wit, M.J., Hart, R.J., Armstrong, R.A., Lindsay, N.M., Sellchop, J.P.F., 1989. Platinum group elements in a 3.5 Ga nickel-iron occurrence: possible evidence of a deep mantle origin. Journal Geophysical Research 94, 795–813.
Van Kranendonk, M.J., Morant, P., 1998. Revised Archaean stratigraphy of the North Shaw 1:100 000 sheet, Pilbara Craton. Geological Survey Western Australia Annual Report 1997, 55–62.
Viloen, R.P., Viljoen, M.J., 1971. The geological and geochemical evolution of the Onverwacht Group in the Barberton Mountain Land, South Africa. Geological Society Aystralia Special Publication 3, 133–151.
Wilhelms, D.E., 1987. The geological history of the Moon. United States Geological Survey professional Paper 1348.
Windley, B.F., 1977. The Evolving Continents. John Wiley & Sons, London.